CURRENT TRENDS AND CHALLENGES IN
RFID

Edited by **Cornel Turcu**

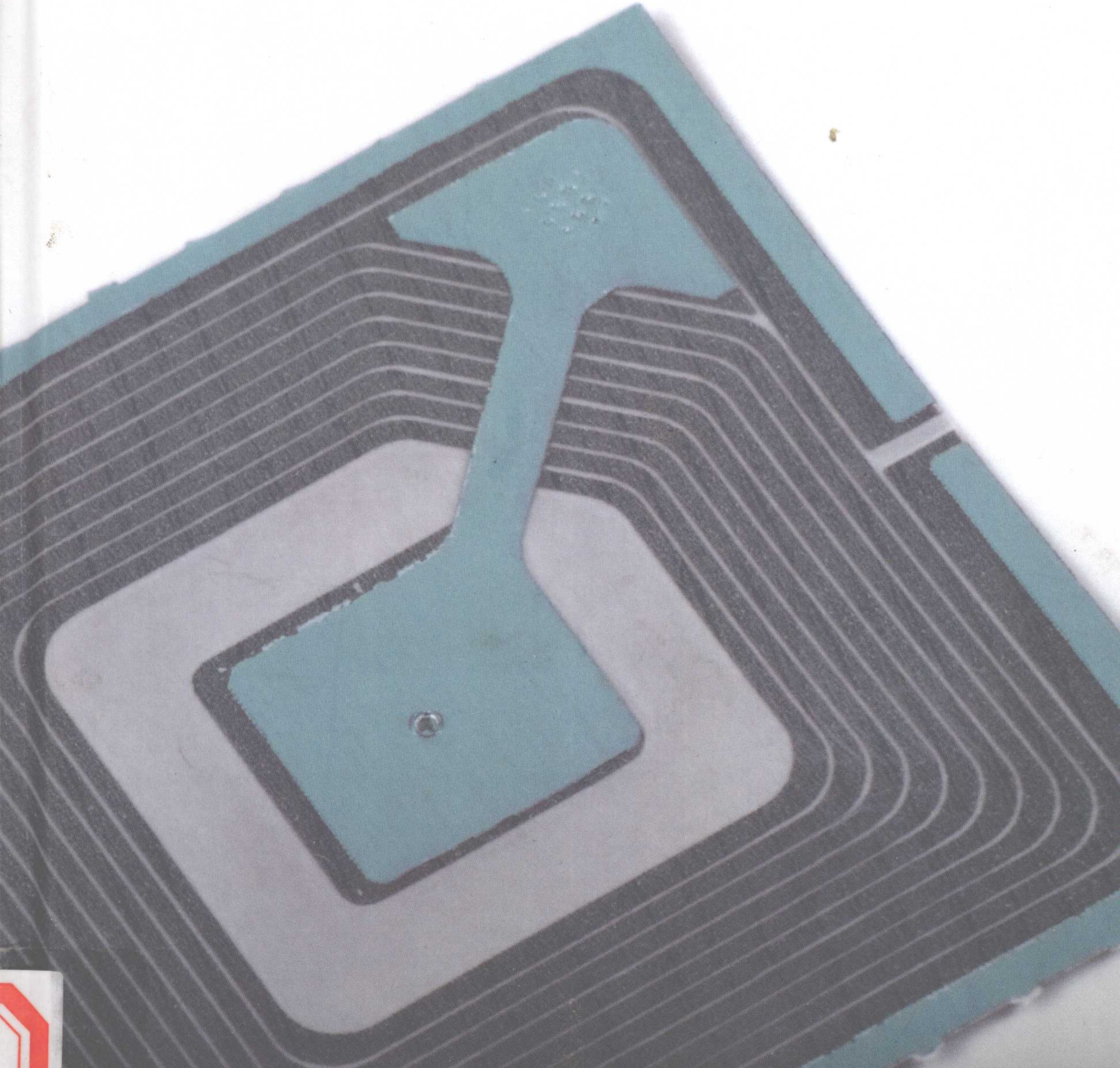

INTECH

INTECH OPEN ACCESS PUBLISHER

INTECH open

free online editions of InTech
Books and Journals can be found at
www.intechopen.com

Current Trends and Challenges in RFID
Edited by Cornel Turcu

Published by InTech
Janeza Trdine 9, 51000 Rijeka, Croatia

Publishing Process Manager Davor Vidic
Technical Editor Teodora Smiljanic
Cover Designer Jan Hyrat
Image Copyright Eric Strand, 2010. Used under license from Shutterstock.com

First published July, 2011
Printed in Croatia

A free online edition of this book is available at www.intechopen.com
Additional hard copies can be obtained from orders@intechweb.org

Current Trends and Challenges in RFID, Edited by Cornel Turcu
p. cm.
ISBN 978-953-307-356-9

Preface

Radio-frequency identification (RFID) is a technology that uses communication through radio waves to transfer data between a reader and an electronic tag attached to an entity for the purpose of identification, tracking and surveillance. Unlike other identification technologies such as barcodes, RFID technology offers several key benefits such as no line-of-sight necessity, robustness, speed, bidirectional communication, reliability in tough environments, bulk detection, superior data capabilities, etc. Because of this, RFID has become particularly successful for a wide area of applications where traditional identification technologies are inadequate for recent demands: inventory tracking, supply chain management, automated manufacturing, healthcare, etc. As the RFID technology is being spread and applied to real world system, RFID systems have received considerable attention from researchers, engineers and industry personnel. As a result of years of research, a lot of literature has been published on the design and use of the RFID systems, covering a wide range of topics: hardware and software, protocols and algorithms, applications, etc.

This book presents some of the most recent research results of RFID users interested in exchanging ideas on the present development issues of and future trends in RFID technology. It consists in a collection of 24 chapters distributed in 5 parts: RF/RFID Backgrounds, Antennas/Tags, Readers, Protocols and Algorithms, and finally, Case studies/Applications.

The book starts with some background chapters related to Radio Frequency (*Chapter 1*), main RF structures (*Chapter 2*) and RF CMOS (*Chapter 3*). Also, this section contains a chapter that deals with structural design of a CMOS voltage regulator for an implanted device (*Chapter 4*).

The second section of the book focuses on antennas and tags. First, some perspectives and technical considerations of microstrip antennas for multi-band RFID reader are presented (*Chapter 5*). Also, the high gain dual-band antennas and limitations have been described. *Chapter 6* includes low-cost solution for RFID tags in terms of design and manufacture considering that applying the traditional printing technologies to produce the antennas will lower the cost of the antenna part. *Chapter 7* deals with conductive adhesives such as the ultralow cost RFID tag antenna material and includes results which are based on the screen printing method, which is very representative at the stage of lab prototyping. *Chapter 8* is a true experimental research in nature and aims to investigate the process consistency and accuracy of printing RFID tag antennas via the screening printing method with a conductive ink, silver-based (Ag) ink, on PET, PVC, and Wet Strength paper. *Chapter 9* presents a novel CPW-fed-slot antenna on artificial magnetic conductor (AMC) combination prototype suitable to be used in 5.8 GHz RFID tags on metallic objects. The last chapter of this section (*Chapter 10*) proposes a guideline for the design of a new kind of RFID tag to be used in each step of the pharmaceutical supply chain. It describes the main features of the pharmaceutical scenario, mainly focusing on item-level tracing systems and RFID devices' performance.

The third section of the book is dedicated to RFID readers. In *Chapter 11* the authors present a demodulation structure suitable for a reader baseband receiver in a passive RFID environment. *Chapter 12* introduces a new reader obtained by adding HDX functionality to an existing FDX reader, together with some design issues that influence reader performance.

After the chapters focusing on readers design, the following chapters present certain aspects related to protocols and algorithms. In *Chapter 13* the authors propose a new scalable authentication protocol for low-cost RFID systems, for which features are presented, both from the tag's and reader's perspective. *Chapter 14* focuses on an RFID model for simulating framed slotted ALOHA based anti-collision protocol for multi-tag identification. *Chapter 15* describes the implementation of direct sequence code division multiple access channel access methods for the UHF-RFID uplink. *Chapter 16* illustrates an unconditionally secure lightweight RFID authentication protocol with untraceability. *Chapter 17* deals with the application of Monte Carlo method for determining the interrogation zone in anti-collision Radio Frequency. In *Chapter 18*, in order to mitigate the influence of the NLOS propagation, the authors propose an iterative delay compensation algorithm based on NEWTON algorithm which improves the accuracy of positioning items using the DCF and shift vector compensation algorithm. Finally, in *Chapter 19*, an efficient spatial range query method is designed for compensating the lost spatial relationship by the linear mapping mechanisms. The experiments conducted on real data sets demonstrate that the proposed approach is efficient and scalable.

The fifth section of the book includes 5 chapters that describe several RFID applications and studies. *Chapter 20* presents some studies on secure RFID authentication and access control, while *Chapter 21* shows an overview of attacks on the HF physical layer of contactless and RFID systems. *Chapter 22* proposes an effective tag movement direction detection method. *Chapter 23* presents a distance measurement and position estimation application in order to evaluate a WSN system. Finally, in *Chapter 24*, cross-layer design is presented as an attractive tool to optimize RFID platforms. The proposed framework for design of RFID platforms can be potentially used for a wide variety of PHY and MAC algorithms under a cross-layer philosophy.

By presenting design issues related to each component of an RFID system, this book reaches its goal, that of being a collection of actual research results and challenges in RFID domain. It completes a collection of RFID books published by Intech, a collection that is a valuable tool for engineers, researchers and industry personnel, either those that are already familiar with RFID or new to this field.

Cornel Turcu
University of Suceava
Romania

Contents

Part 1

RF/RFID Backgrounds

1

Radio Frequency Background

Tales Cleber Pimenta, Paulo C. Crepaldi and Luis H. C. Ferreira
Universidade Federal de Itajuba
Brazil

1. Introduction

Design considerations for the traditional low frequency circuits and the RF circuits are quite different. In low frequency design, the maximum signal transfer occurs when the source presents low impedance while the load presents high impedance. A typical example is a buffer, where the input impedance is high and the output impedance is low. As long as that requirement is fulfilled, the designer is capable of choosing arbitrary levels of impedance that best suits the circuit requirements or applications.

Therefore this chapter aims to provide background on impedance matching between source and load, with or without a transmission line. The analysis can be conducted by using Smith Charts and S-Parameters, which are also presented in this chapter. The analysis in this chapter is oriented to RFID applications whereas other books provide general analysis.

During RF design, the impedances should be matched for maximum signal transfer. Additionally, when the circuits are connected using transmission lines, they should match also the standard values of the transmission lines. At very low frequencies, transmission lines can be thought as just a wire. Nevertheless, at high frequencies, the signal wavelength is comparable to or smaller than the length of the transmissions line and power can be seen as traveling waves. As a matter of fact, even a conductor can be thought as a transmission line in a high frequency circuit.

Most RF equipments and coaxial cables use the standard impedances of 50 or 75 Ω. The value of 75 Ω is used, as an example, in cable TV equipment, since this value provides the minimum losses, as it is desired in transmitting the signal over long distances. In fact, the value of impedance for minimum loss should be 77 Ω, but it was rounded to 75 Ω by convenience.

The value of 50 Ω corresponds to a reasonable compromise, the average, between the minimum loss of a 77 Ω and the maximum power handling capability given of 30 Ω.

2. Transmission line

Fig. 1 shows the lumped component model of a real (lossy) transmission line. The segment indicated corresponds to an infinitesimal segment of the transmission line. The characteristic impedance Z_0 of this line can be found to be [1]:

$$Z_0 = \sqrt{\frac{Z}{Y}} = \sqrt{\frac{R + j\omega L}{G + j\omega C}} \tag{1}$$

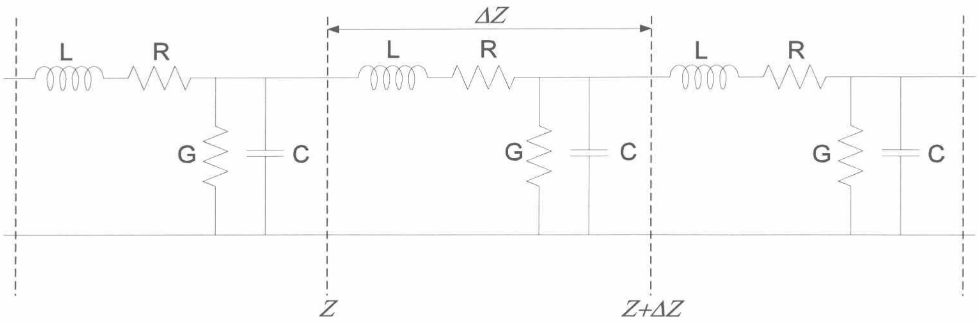

Fig. 1. Lumped component model of a transmission line.

As can be observed, the characteristic impedance Z_0 is dependent on the frequency. Nevertheless, if the resistive terms R and G are negligible, the expression of the characteristic impedance Z_0 can be simplified to:

$$Z_0 = \sqrt{\frac{L}{C}} \tag{2}$$

If the value of RC is equal to GL, expression (1) yields the same value of expression (2). In other words, choosing the L/R time constant of the series impedance equals to the C/G time constant, a lossy line will behave as a lossless line, so that its characteristic impedance will be independent of the frequency[1].

2.1 Reflection coefficient

If a transmission line is terminated by an impedance Z_0, then a signal traveling down the line with a ratio of voltage to current equal to Z_0 will maintain its ratio upon encountering the load and there will be no reflections. On the other hand, when the load is different of Z_0, then it imposes its own particular ratio of voltage to current, and the only way to reconcile the conflict is by having some of the signal reflected back towards the source. In order to distinguish the incident and the reflected signals, the subscripts i and r, respectively, will be used.

The incident signal is given by:

$$Z_0 = \frac{E_i}{I_i} \tag{3}$$

At the load end, the mismatch in impedances gives rise to a reflected signal. Since the system is still linear, the total voltage at any point in the system is the sum of incident and reflected voltages. The net current is superposition of incident and reflected currents. However, since the currents are traveling in opposite directions, the net current is the difference between them. Therefore, the load impedance is given by:

$$Z_L = \frac{E_i + E_r}{I_i - I_r} \tag{4}$$

Expression (4) can be rewritten to express Z_L as function of Z_0 as:

$$Z_L = \frac{E_i + E_r}{I_i - I_r} = \frac{E_i}{I_i}\left[\frac{1 + E_r / E_i}{1 - E_r / E_i}\right] = Z_0\left[\frac{1 + E_r / E_i}{1 - E_r / E_i}\right] \tag{5}$$

The ratio of reflected to incident quantities at the load end of the line is called Reflection Coefficient Γ_L. Therefore, expression (5) can be rewritten as:

$$Z_L = \frac{E_i + E_r}{I_i - I_r} = Z_0\left[\frac{1 + \Gamma_L}{1 - \Gamma_L}\right] \tag{6}$$

Solving for Γ_L yields:

$$\Gamma_L = \frac{Z_L - Z_0}{Z_L + Z_0} \tag{7}$$

As can be observed from expression (7), if the impedances of the load and the line are equal, there will be no reflection. If the line is terminated in either a short or an open circuit, the reflection will be maximum, with a magnitude of 1 [1].

Therefore, if a transmission line is terminated by its characteristic impedance there will be no reflection since all the transmitted power is absorbed by the load and the energy flows in just one direction.

When the line is terminated by a short circuit a reflected wave is sent back to the source since the short can not sustain any voltage, and therefore dissipates zero power. The incident and the reflected voltage waves are of the same magnitude. They are 180º out of phase at the load and they travel in opposite directions.

If the line is terminated by an open circuit a reflected wave is sent back to the source since the open can not sustain any current, and therefore dissipates zero power. The incident and the reflected current waves are of the same magnitude and travel in opposite directions. The current waves are 180º out of phase at the load, but the incident and reflected voltage waves are in phase [1].

If the line is terminated by an impedance different of the short, open and characteristic impedance, part of the signal will be absorbed by the load and part will be reflected back. The amount of reflected signal is given by expression (7).

3. Smith chart

The reflection coefficient Γ_L of expression (7) was obtained from expression (6). By the same way, solving for Z_L in expression (7) yields Γ_L, thus forming a mapping of one complex number into another. The relationship between these two complex numbers forms a bilinear transformation, which means that knowing one is equivalent to knowing the other.

Since Z_L can have any value and $|\Gamma_L|$ cannot exceed unity for passive loads, it is therefore much more convenient plotting Γ_L than plotting Z_L.

The reflection coefficient can become even more convenient by normalizing it to Z_0, as:

$$\Gamma = \frac{\frac{Z_L}{Z_0} - 1}{\frac{Z_L}{Z_0} + 1} = \frac{Z - 1}{Z + 1} \tag{8}$$

On the same way, normalizing (6) results in:

$$Z = \frac{1+\Gamma}{1-\Gamma} \tag{9}$$

Considering the normalized real and imaginary parts of both Γ and Z then:

$$Z = R + jX = \frac{1+\Gamma}{1-\Gamma} = \frac{1+\Gamma_r + j\Gamma_i}{1-\Gamma_r - j\Gamma_i} \tag{10}$$

After some algebraic manipulation (using conjugate), the real and imaginary parts are of Z are:

$$R = \frac{1-\Gamma_r^2-\Gamma_i^2}{1+\Gamma_r^2-2\Gamma_r+\Gamma_i^2} \tag{11}$$

$$X = \frac{2\Gamma_i}{1+\Gamma_r^2-2\Gamma_r+\Gamma_i^2} \tag{12}$$

Expression (11) can be manipulated as:

$$\begin{aligned}
&R + R\Gamma_r^2 - 2R\Gamma_r + R\Gamma_i^2 = 1-\Gamma_r^2-\Gamma_i^2\\
&R\Gamma_r^2 - 2R\Gamma_r + R\Gamma_i^2 + \Gamma_r^2 + \Gamma_i^2 = 1-R\\
&R\Gamma_r^2 - 2R\Gamma_r + R\Gamma_i^2 + \Gamma_r^2 + \Gamma_i^2 = (1-R)\frac{(1+R)}{(1+R)}\\
&R\Gamma_r^2 - 2R\Gamma_r + R\Gamma_i^2 + \Gamma_r^2 + \Gamma_i^2 = \frac{1}{(1+R)} - \frac{R^2}{(1+R)}\\
&\Gamma_r^2(1+R) - 2R\Gamma_r + \frac{R^2}{(1+R)} + \Gamma_i^2(1+R) = \frac{1}{(1+R)}\\
&\Gamma_r^2 - 2\Gamma_r\frac{R}{(R+1)} + \frac{R^2}{(1+R)^2} + \Gamma_i^2 = \frac{1}{(1+R)^2}\\
&\left(\Gamma_r - \frac{R}{R+1}\right)^2 + \Gamma_i^2 = \left(\frac{1}{1+R}\right)^2
\end{aligned} \tag{13}$$

Similarly, expression (12) into:

$$\left(\Gamma_r - 1\right)^2 + \left(\Gamma_i - \frac{1}{X}\right)^2 = \frac{1}{X^2} \tag{14}$$

When the two parametric equations (13) and (14) are drawn on a complex coordinate, they build the Smithchart. Equation (13) forms resistance circles, and equation (14) generates reactance circles, as shown in Fig. 2 and Fig. 3, respectively. The resulting Smithchart is illustrated in Fig. 4.

As can be verified from expression (13), the imaginary axis in the Z-plane (resistance equals 0) is mapped as a unity circles into Γ-plane. The other lines of constant resistance in the Z-plane are also mapped as circles, but of different diameter in the Γ-plane. Nevertheless, they are all tangent at the point $\Gamma=1$, as shown in Fig. 2. The larger the value of the resistance, the smaller becomes the circle [1, 2].

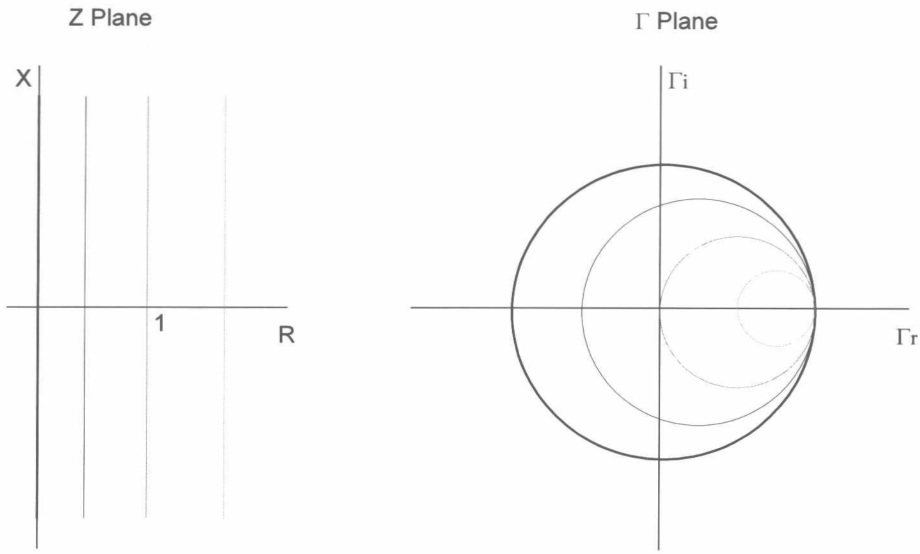

Fig. 2. Mapping of Z-plane into Γ-plane for constant resistances.

As can be verified from expression (14), lines of constant reactance are perpendicular to lines of constant resistance in the Z-plane. This same orthogonality is preserved in the Γ-plane by having arcs perpendicular to the constant resistance lines, as indicated in Fig. 3.

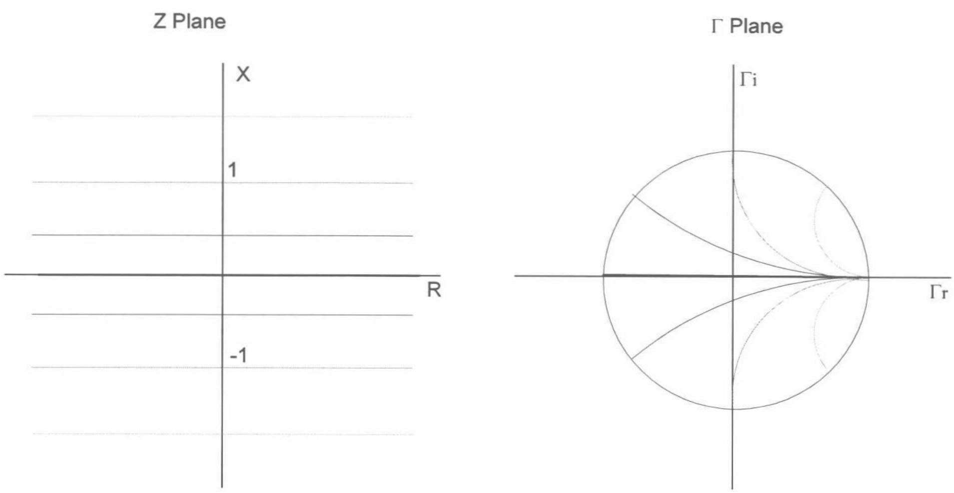

Fig. 3. Mapping of Z-plane into Γ-plane for constant reactances.

The Smith, as shown in Fig. 4, is just the plotting of both constant resistance and constant reactance, but without the presence of the Γ axes. The center of the Smith chart corresponds to zero reflection (Z_L equals Z_0)[1].

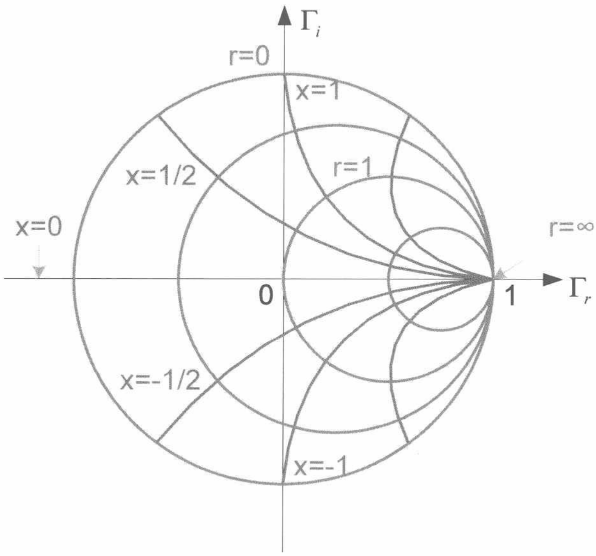

Fig. 4. Smith chart.

The upper half of the Smith chart corresponds to the upper half part of the Z-plane, and therefore presents inductive loads. On the same way, the bottom half of the Smith chart corresponds to the bottom half part of the Z-plane, thus representing capacitive loads. Obviously, the Re axis of the Smith chart represents purely resistive loads.
Although the Smith chart presents many interesting and useful properties, they will no be presented here due to the focus of this material.

2.1 Admittance chart

The Smithchart is built by considering impedance (resistance and reactance). Once the Smithchart is developed, a similar approach can be used for admittance analysis. The concept that admittance is the inverse of impedance is very important for parallel circuit synthesis. Adding new elements in series can be resolved easily by adding the impedance values. However, summing elements in parallel can be cumbersome in terms of impedance. Thus, admittance is often considered for parallel elements.
By definition, admittance is expressed as:

$$Y = \frac{1}{Z} = G + jB \tag{15}$$

where G is conductance and B is susceptance of the element. The reflection coefficient Γ can be expressed in terms of normalized admittance as: